Understanding the geometric and electronic factors of PtNi bimetallic surfaces for efficient and selective catalytic hydrogenation of biomass-derived oxygenates

Wu, Jingcheng; Liu, Chuangwei; Zhu, Yuting; Song, Xiangbo; Wen, Chengyan; Zhang, Xinghua; Wang, Chenguang; Ma, Longlong

Published in:
Journal of Energy Chemistry

Link to article, DOI:
10.1016/j.jechem.2020.12.011

Publication date:
2021

Document Version
Peer reviewed version

Journal Pre-proofs

Understanding the geometric and electronic factors of PtNi bimetallic surfaces for efficient and selective catalytic hydrogenation of biomass-derived oxygenates

Jingcheng Wu, Chuangwei Liu, Yuting Zhu, Xiangbo Song, Chengyan Wen, Xinghua Zhang, Chenguang Wang, Longlong Ma

PII: S2095-4956(20)30811-1
DOI: https://doi.org/10.1016/j.jechem.2020.12.011
Reference: JECHEM 1725

To appear in: *Journal of Energy Chemistry*

Received Date: 27 November 2020
Revised Date: 10 December 2020
Accepted Date: 10 December 2020

Please cite this article as: J. Wu, C. Liu, Y. Zhu, X. Song, C. Wen, X. Zhang, C. Wang, L. Ma, Understanding the geometric and electronic factors of PtNi bimetallic surfaces for efficient and selective catalytic hydrogenation of biomass-derived oxygenates, *Journal of Energy Chemistry* (2020), doi: https://doi.org/10.1016/j.jechem.2020.12.011

Understanding the geometric and electronic factors of PtNi bimetallic surfaces for efficient and selective catalytic hydrogenation of biomass-derived oxygenates

Jingcheng Wu [a,c,d,e,1], Chuangwei Liu [b,1], Yuting Zhu [a,c,d,e], Xiangbo Song [a,c,d,e], Chengyan Wen [a,c,d], Xinghua Zhang [a,c,d], Chenguang Wang [a,c,d,*], Longlong Ma [a,c,d]

[a] *Guangzhou Institute of Energy Conversion, Chinese Academy of Sciences, Guangzhou 510640, Guangdong, China*

[b] *Department of Energy Conversion and Storage, Technical University of Denmark, Lyngby, 2800, Denmark*

[c] *Key Laboratory of Renewable Energy, Chinese Academy of Sciences, Guangzhou 510640, Guangdong, China*

[d] *Guangdong Provincial Key Laboratory of New and Renewable Energy Research and Development, Chinese Academy of Sciences, Guangzhou 510640, Guangdong, China*

[e] *University of Chinese Academy of Sciences, Beijing 100049, China*

[1] These authors contributed equally to this work.

*Corresponding author.

Email address: wangcg@ms.giec.ac.cn (C. Wang)

Abstract

Ni-base catalysts are promising candidate for the hydrogenation of furfural (FAL) to high-value chemicals. However, slow intermediate desorption and low selectivity limit its implementation. Identifying the catalytic performance of each active sites is vital to design hydrogenation catalyst, and tuning the geometrical sites at molecule level in PtNi could lead to the modification of electronic structure, and thus the selective for the hydrogenation of FAL was modulated. Herein, PtNi hollow nanoframes (PtNi HNFs) with three dimensional (3D) molecular accessibility were synthesized, EDX results suggested that Ni was evenly distributed inside of the hollow nanoframes, whereas Pt was relatively concentrated at the edges. DFT calculation demonstrated that PtNi significant decrease the desorption energy of the intermediate. This strategy could not only enhance the desorption of intermediate to improve the catalytic performance, but also transfer the adsorption mode of FAL on catalyst surface to selective hydrogenation of FAL to FOL or THFA. The PtNi HNFs catalyst afforded excellent catalytic performance for selective hydrogenation of a broad range of biomass-derived platform chemicals under mild conditions, especially of FAL to furfuryl alcohol (FOL), in quantitative FOL yields (99%) with high TOF of 2.56 h^{-1}. It is found that the superior performance of PtNi HNFs is attributed to its 3D hierarchical structure and synergistic electronic effects between Pt and

Ni. Besides, the kinetic study demonstrated that the activation energy for hydrogenation of FAL was as low as 54.95 kJ mol^{-1}.

Keywords: PtNi HNFs; Biomass; Hydrogenation; Biofuels; Heterogeneous catalysts

1. Introduction

The overexploitation and depletion of non-renewable fossil source are causing aggravating energy crisis and severe environmental pollution [1–4]. Upgrading of various renewable biomass-derived platform chemicals is a sustainable approach to provide valuable biofuels and high value-added chemicals for human society [5–8]. Furfural (FAL) is a crucial versatile intermediate to manufacture biofuels and high value products, which was directly obtained from enormous potential supply of lignocellulose [9–13]. Especially, the selective hydrogenation of FAL into furfuryl alcohol (FOL) is of great

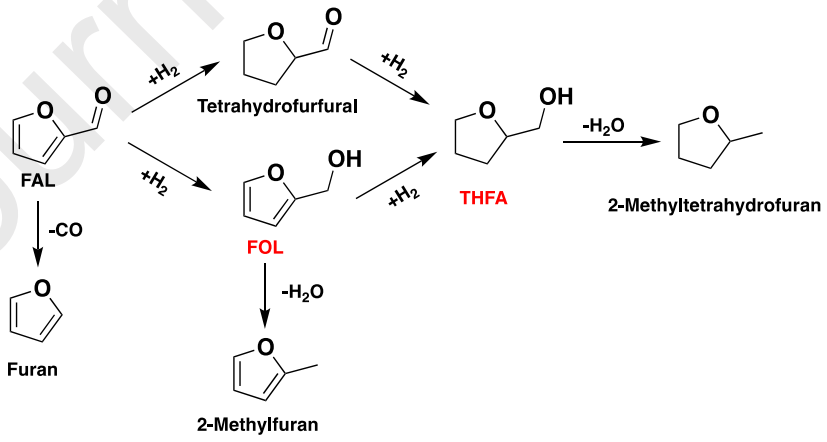

Scheme 1. Reaction pathway for hydrogenation of FAL to FOL or THFA and potential side reactions.

significant value in the biorefinery application because FOL is an important industrial chemical, which was widely employed in the production of crown ethers, artificial fibers, biofuels, and fuel additive [14–16]. It is estimated that 65% of the FAL produced globally each year was converted into FOL for direct transformation into valuable chemicals, such as tetrahydrofurfuryl alcohol (THFA) (Scheme 1) [17,18].

Conventional production of FOL is carried over Cu-Cr catalyst under harsh conditions, i.e. 180 °C, 7–10 MPa H_2 pressure [19]. It is desirable to develop Cr-free catalyst for the production of FOL due to high H_2 pressure, the toxicity of Cr-base catalysts, and the deactivation of catalysts. Ni-base catalysts are known to be effective in hydrogenation of FAL [20]. However, there are two shortcomings in the catalytic hydrogenation of FAL: (1) Ni-base catalysts are excellent in the adsorption and activation of H_2, but the activated H* and the formed intermediates are hard to desorb from the surface of Ni, which will slow the subsequent hydrogenation [21]. (2) A flat adsorption mode of FAL on Ni surface will promote the adsorption and activation of both C=C bond on furan ring and C=O bond, resulting in the total hydrogenation of FAL to THFA [22]. In the previous reports, the electronic structure of Ni (*d*-band) is the major factor in determining the adsorption of H* and FAL on Ni [23,24]. Therefore, weakening the interaction between Ni and H* by tuning the *d*-bands of Ni will be an excellent strategy to promote the desorption of H*, resulting in the alter of adsorption of FAL on Ni [25].

As far as we know, there are few reports on engineering the electronic structure to promote the performance of FAL hydrogenation.

Adding a second metal elemental was a feasible approach towards tuning the electronic structure of Ni-base catalysts, resulting in the bimetallic catalysts with enhanced catalytic performance. Ni-based catalysts such as Ni-Pt [26], Ni-Pd [27], Ni-Cu [28], Ni-Sn [29] and Ni-Co [30] exhibited unique properties compared with their parent metal catalysts. The catalytic performance of bimetallic catalysts (activity and selectivity) is highly dependent on its component and geometry. For exam, Ni_3Sn_2 exhibited an excellent performance in selective hydrogenation of FAL to FOL due to the superior adsorption of −CHO on Ni_3Sn_2 surface [29]. The introduction of Cu to Ni surface enhanced the selectivity and decreased the deactivation rate, which was attributed to the isolation of Ni atoms from another by Cu and thus changed the adsorption mode on Ni [31]. Recent theoretical calculations suggested that Pt-Ni-Pt alloy catalyst was a promising candidate for FAL hydrogenation [26]. In our previous work, we employed a highly dispersed PtNi alloy catalyst that Ni and electron-rich Pt promoted the hydrogenation of FAL to THFA synergistically [32]. However, the rational design of the selective hydrogenation catalyst with desirable electronic and geometric structure is challenge. Moreover, most works are mainly concentrated on the relationship between the catalytic performance and the adsorption mode of FAL, but these for intermediate and H_2 were ignored.

Herein, we synthesized PtNi hollow nanoframes (PtNi HNFs) with three dimensional (3D) molecular accessibility to understand the effect of geometric and electronic structure on the hydrogenation reaction. Extensive characterizations were performed to demonstrate that Ni was evenly distributed inside of the hollow nanoframes, whereas Pt was relatively concentrated at the edges. The PtNi HNFs catalyst was explored to be highly selective catalytic hydrogenation of a variety of biomass-derived carbonyl compounds to alcohols under mild conditions. In addition, the kinetic experiments were carried to reveal the relationship between active sites and their catalytic performances. Theoretical calculation suggested that the desorption of FOL was rate-determining step and smallest desorption energy of FOL on PtNi, which was attributed to the tuning *d*-band of Ni by Pt. Furthermore, the FAL favors to adopt a titled adsorption orientation on PtNi HNFs catalyst while a flat adsorption on Ni, which is beneficial for the selective hydrogenation of FAL to FOL. This study provides a deep insight into effect and selective catalyst for FAL hydrogenation.

2. Experimental

2.1. Catalyst synthesis

Raw wooden active carbon was purchased from Sunson Activated Carbon Technology CO., Ltd. Nitric acid (HNO_3) was purchased from Tianjin Fu Chen Chemical Reagents Factory. $H_2PtCl_6 \cdot 6H_2O$ and $Ni(NO_3)_2 \cdot 6H_2O$ were purchased from Shanghai

Macklin Biochemical Co., Ltd. The pre-treated raw wooden active carbon, Pt/C, Ni/C and PtNi/C catalyst were prepared as our previous work [33].

PtNi HNFs were prepared by a literature method with minor modification [34]. 20 mg $H_2PtCl_6 \cdot 6H_2O$ and 17.5 mg $Ni(NO_3)_2 \cdot 6H_2O$ were added in 0.4 mL deionized water to form a transparent solution. Then, the solution was added to 10 mL oleylamine in a three-necked flask and heated the temperature to 160 °C, and then kept for 3 min to remove deionized water. After that, the temperature was heated up to 270 °C under Ar atmosphere. After 3 min, the transparent solution turned into a black slurry, the reaction was stopped and cool to room temperature. The PtNi precursor was collected by centrifugation (8000 rpm) for 5 min. PtNi precursor was then dispersed into a solution mixed 5 mL chloroform and 0.2 mL oleylamine. The colloidal solution was diluted with 10 mL hexadecane and sonicated for 20 min, then the solution was heated to 120 °C for 12 h. The afforded PtNi HNFs was collected by centrifugation (8000 rpm) for 5 min. The PtNi HNFs was supported on the pre-treated active carbon by wet impregnation. 1 g of pre-treated active carbon was added in 10 mL water and 10 mL ethanol, and the mixture was stirred for 30 min. Then PtNi HNFs solid was added to the active carbon solution and stirred for 24 h at room temperature. The catalyst was dried at 60 °C overnight and then the support catalyst was subsequent thermal treatment in inert gas (Ar) at 400 °C.

2.2. Activity tests

Typically, 20 mL of solvent, 0.2 g of furfural and 0.1 g of catalyst were loaded into

a 50 mL reactor (Anhui Kemi Machinery Technology Co., Ltd., Anhui, China; MS100-P5-T4-HC1-SV). Firstly, the reactor was flushed with N_2 three times to remove air, and then flushed with desired pressure H_2. Then the reaction was performed at a pre-set temperature. The stirring rate of the reaction rate is 600 r/min at each experiment. After the reaction, the reactor was cooled to room temperature. The gas phase was collected by a gas bag for analysis, and liquid solution was separated by centrifugation.

2.3. Products analysis

The gas phase product was measured by a gas chromatograph (GC) equipped with a thermal conductivity detector (TCD) and a flame ionization detector (FID) by an external standard method. The organic phase was analyzed by gas chromatography (GC) which equipped with an FID detector. The oven temperature was increased to 60 °C from room temperature for 2 min, and then ramp to 200 °C with 10 °C/min and hold for 10 min. Helium was the carrier gas with split ratio of 5:1. The FAL conversion and FOL yield were measured by the following equations:

$$\text{FAL conversion} = \frac{\text{Initial mole of FAL - Final mole of FAL}}{\text{Initial mole of FAL}}$$

$$\text{FOL yield} = \frac{\text{Mole of product}}{\text{Theoreticle mole of product}}$$

$$\text{TOF} = \frac{\text{Mole (converted FAL)}}{\text{Mol (total metal added)} \times \text{reaction time (h)}}$$

2.4. Characterization of catalyst

The PtNi HNFs was characterized by X-ray Diffraction (XRD), X-ray Photo-electronic Spectroscopy (XPS), Search Engine Marketing (SEM), Transmission Electron Microscope (TEM), and Brunner-Emmet-Teller (BET). N_2 adsorption isotherms

of the PtNi HNFs were performed on a Micromeritics ASAP 2020 instrument. Firstly, the sample was degassed at 200 °C for 4 h. The surface area was evaluated by BET method and the average pore volume and pore size were analyzed by BJH method. XPS was measured on a Leybold LH 10 spectrometer equipped with a single-channel detector, employing Mg K_α radiation. For the analysis of the XPS peaks, the C1s peak position was set at 284.5 eV and used as reference to locate the other peaks. XRD was carried on a Rigaku diffractometer using Cu K radiation (λ = 0.1543 nm, 40 kV, 30 mA). The structure and morphology of the PtNi HNFs were studied by scanning TEM and SEM equipped with an EDS analyzer operated at 200 kV.

3. Results and discussion

3.1. Characterization of the catalysts

The Pt/C, Ni/C and PtNi/C catalysts were characterized in our previous work [32]. The morphological features and crystalline structure of PtNi HNFs were studied by SEM and TEM. The SEM and TEM images in Fig. 1(A–C) clearly showed that PtNi HNFs had a uniform rhombic dodecahedron morphology which was hollow nanoframes with unchanged symmetry and the particle size of PtNi HNFs was 30~50 nm. HRTEM suggested that PtNi HNFs catalysts were face centered cubic (fcc) nanocrystals and the parent rhombic dodecahedron maintained single crystalline structure (Fig. S1). Additionally, the pattern of PtNi HNFs exhibited the crystal planes of (111), (200) and (220) corresponding to the single crystalline structure of the hollow nanoframes (Fig. S1).

169 The single crystalline structure of the hollow nanoframes was further proved by XRD
170 patterns (Fig. 1H). The three main bands (111), (200) and (220) were located between Pt
171 and Ni and the PtNi HNFs were fcc, suggesting the formation of PtNi HNFs. The PtNi
172 HNFs were Pt-rich at edge and Ni concentrated inside which could be proved by the
173 EDX results, where the peak was in a low angle (high d spacing) and the weight ratio of
174 Pt: Ni was 2.5:1 on the catalyst surface (Fig. S2).

175 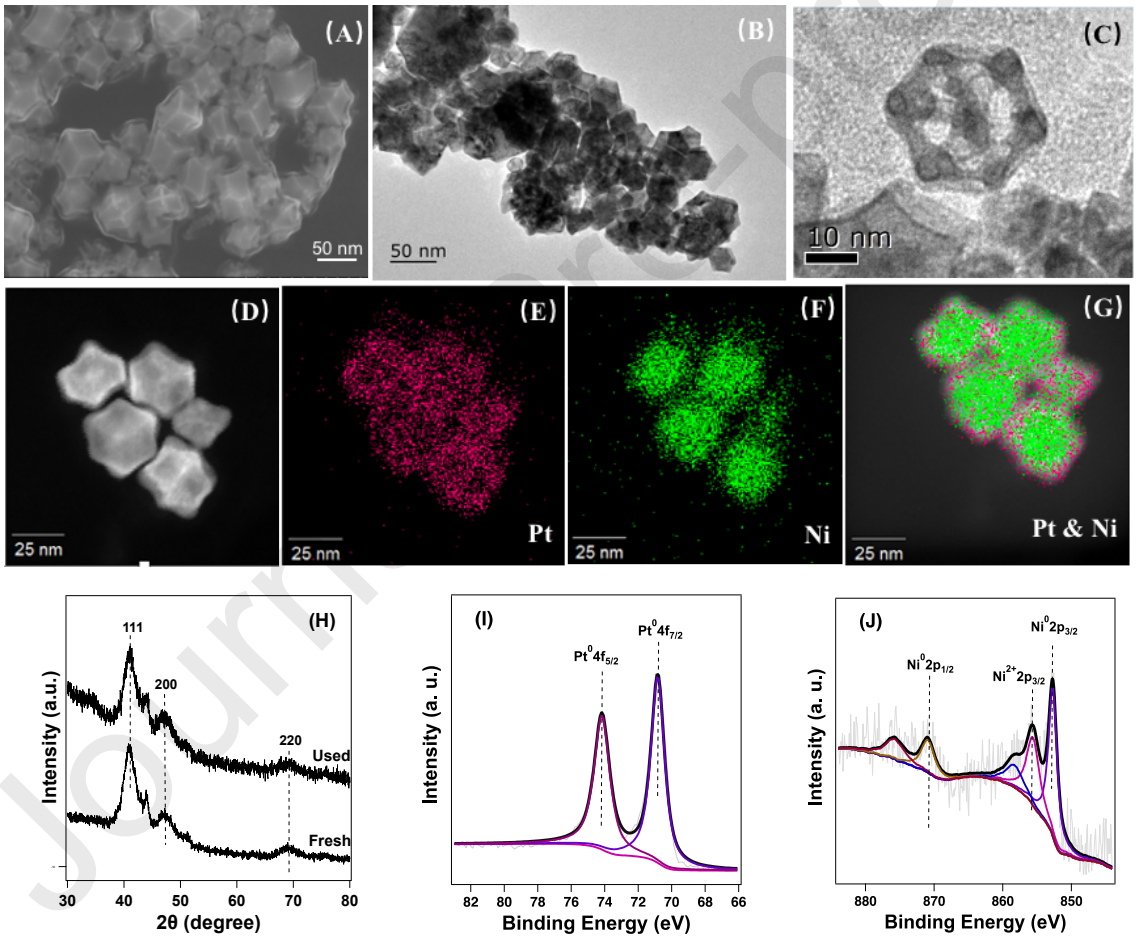

176

177 **Fig. 1.** (A) SEM image of PtNi HNFs; (B and C) TEM images of PtNi HNFs; (D) EDX mapping of
178 PtNi HNFs (E) Pt, (F) Ni and (G) reconstructed overlay maps (Pt and Ni). (H) XRD pattern of used
179 and fresh PtNi HNFs; XPS spectra of (I) Pt4f and (J) Ni2p level on PtNi HNFs.

180

The structural parameters of the supported catalysts were shown in Table S1. The surface area of PtNi HNFs was smaller than Pt/C and Ni/C catalysts while higher than PtNi/C catalyst.

The oxidation state of PtNi HNFs was characterized by X-ray Photoelectron Spectroscopy (XPS). Characteristic peaks with binding energies of 70.4 and 74.2 eV corresponding to the Pt^0 $4f_{7/2}$ and Pt^0 $4f_{5/2}$, respectively, indicating that most Pt are in metallic form (Fig. 1I). Strong peaks for Ni^0 $2p_{3/2}$ (852.8 eV) and Ni^0 $2p_{1/2}$ (870.8 eV) were observed, suggesting most Ni was present as metal (Fig. 1J). There is still a peak for the $2p_{3/2}$ (855.8 eV), which suggests that roughly one-third of Ni are present as Ni^{2+}. Based on the electronegativity of elements Ni (1.91) and Pt (2.28), it is expected to observe the charge transfer from Ni to Pt, which suggests that Pt could attract electrons from Ni and thus Ni remains in Ni^{2+} state [35]. As we all know, bonding energy decreased with an increase in the electron density on metal. Based on this theory, the XPS results demonstrated that Pt is electron richer than in monometallic Pt/C catalyst.

3.2. Hydrogenation of FAL over various catalysts

196 Hydrogenation of FAL was chosen as model reaction to probe the relationship
197 between the electronic and geometric structure, and their performance over Pt/C, Ni/C,
198 PtNi/C and PtNi HNFs catalysts. As shown in Fig. 2, the blank run indicated that only a
199 small amount of FAL (6%) was converted without FOL formation in the absence of metal
200 catalyst in isopropyl alcohol (IPA) at 100 °C for 1 h, suggesting the active carbon was not
201 active in the hydrogenation. The main side product is furfural diisopropyl acetal (FDIA),
202 which derived from acetalization of FAL with isopropyl alcohol. When the

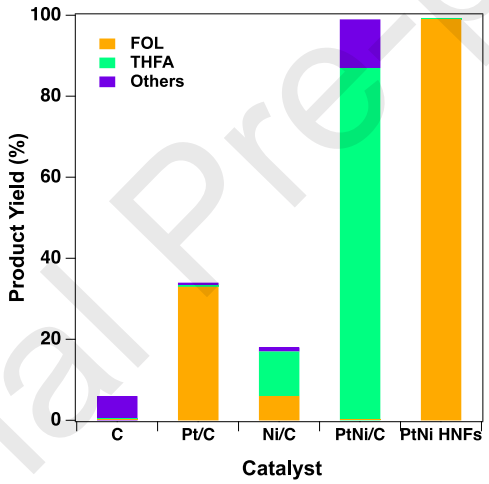

Fig. 2. Effect of monometallic and bimetallic catalysts on hydrogenation of FAL. Reaction condition: FAL, 0.2 g; weight of catalyst, 0.1 g; isopropyl alcohol, 20 mL; 100 °C, 1 h; 1 MPa H_2 was charged at room temperature;

203 hydrogenation reaction was performed in IPA at 100 °C over Pt(3)/C, 34% FAL
204 conversion with 33% FOL yield (0.48 h^{-1} TOF) was obtained. Moreover, Ni(3)/C
205 catalyst only gave 6% FOL yield and 11% THFA yield with 18% conversion of FAL
206 (0.24 h^{-1} TOF). Gratifyingly, when PtNi alloy catalyst with high small spherical particle
207 (8–10 nm) was employed, 87% THFA yield was obtained. The main side product was

208 2-methylfuran (11%) via hydrogenolysis reaction. Ni alone gave lower FOL selectivity
209 and Pt alone exhibited a low FAL conversion than PtNi catalyst, suggesting that Pt and
210 Ni metals facilitate enhancement of the activity in a synergetic way [32]. Ni-base
211 catalysts were excellent in the adsorption and activation of H_2, but the activated H* and
212 intermediate were hard to desorb from the surface of Ni, which will slow the subsequent
213 hydrogenation. The electronic structure of Ni (*d*-band) is the major factor in determining
214 the adsorption H* and FAL on Ni. Adding second metal Pt will tune the electronic
215 structure of Ni-base catalysts, resulting in the enhancement of catalytic performance. This
216 is demonstrated by the previous works, several metals were employed to form bimetallic
217 catalysts and the plot showed that metal Ni have optimal effect in tuning the binding
218 energy of oxygen-containing species on Pt [36,37]. It is interesting to see when PtNi
219 HNFs catalyst was employed in the hydrogenation of FAL, 99% FAL conversion and
220 99% FOL yield (2.56 h^{-1} TOF) was obtained. Changing the geometry of PtNi catalyst to
221 PtNi HNFs catalyst with hollow rhombic dodecahedron morphology increased the
222 selectivity for semi hydrogenation pathway at the expense of the total hydrogenation
223 pathway. The detail mechanism will be discussed in Section 3.8.

224 *3.3. Solvent effect*

The hydrogen donor is gas hydrogen rather than proton solvents (alcohols or organic acid) and hydrogen pressure is indispensable rather than total pressure in the reactor at low temperature. A control experiment was carried with 2 MPa N_2 pressure in IPA, only 6% FAL conversion without FOL formation at 50 °C. The main side product is furfural diisopropyl acetal (FDIA), which produced from the acetalization of FAL with IPA. To further understand the role of IPA in the hydrogenation reaction at higher temperature, experiments were carried at 100 °C and 150 °C with N_2. When the reaction was performed at 100 °C, 8% FAL conversion without FOL was observed, suggesting some undesired side reaction in the absence of H_2. However, 12% FAL conversion and 12% FOL yield were observed when the reaction was conducted at 150 °C, indicating IPA could act as hydrogen donor at 150 °C rather than 100 °C. It is reported that alcohols can

Table 1. The effect of solvents on hydrogenation of FAL

Entry	Solvents	*T* (°C)	Pressure (MPa)	Conv. (%)	Yield (%)
1	IPA	50	2, N_2	6	0
2	IPA	100	2, N_2	8	0
3	IPA	100	2, H_2	99	99
4	IPA	150	2, N_2	12	12
5	Methanol	100	2, H_2	68	48
6	Ethanol	100	2, H_2	56	52
7	Cyclohexanol	100	2, H_2	7	5
8	2-butanol	100	2, H_2	38	35
9	Toluene	100	2, H_2	10	8
10	Water	100	2, H_2	38	38
11	Water	50	2, H_2	16	16
12	IPA	50	2, H_2	48	48
13	50% IPA & 50% water	50	2, H_2	87	87

Reaction condition: Weight of catalyst, 0.1 g; solution, 20 mL; 1 MPa H_2 was charged at room temperature.

be used as hydrogen donors at high temperatures (usually higher than 150 °C) and therefore solvent (IPA in this paper) is not contributing hydrogen towards the reaction at 100 °C [38]. In the next experiments, the temperature was carried at 100 °C to avoid the solvent donor effect. To further understand the effect of solvent on the reaction, experiments were performed at 100 °C for 1 h with different solvents. As shown in Table 1, 99% FOL yield with 99% FAL conversion was achieved within 1 h in IPA. The difference in activity may due to the Hansen Solubility Parameter (HSP) of solvents, which are shown in Table S2. FAL and FOL have the HSP value of 22.9 and 25.6, respectively. The IPA has a medium HSP value between FAL and FOL which means FAL is favored to be reduced in IPA. Besides, it is presumably due to excellent transfer hydrogenation ability of IPA that would augment possible contribution during the reaction in the presence of hydrogen.

It is worth mentioning that water is a green and cheap solvent than organic solvents in the hydrogenation reaction. When the hydrogenation reaction was carried in water at 50 °C, only 16% FAL conversion was obtained, the low FAL conversion is due to the adsorption of FAL on the hydrophobic catalyst was prevented by water (entry 11). However, 100% FOL selectivity was obtained, suggesting water is favored to prevent the side reaction, such as the acetalization of FAL with alcohols. Increasing temperature to 100 °C, 38% FAL conversion was obtained at high temperature, suggesting the adsorption of FAL on hydrophobic catalyst is highly dependent on temperature (entry 10). To confirm the effect of water on the hydrogenation of FAL, the mixture of IPA and

water were employed as the solvent at 50 °C, a significant increase in the FAL conversion and FOL yield compared with pure water or IPA, suggesting water played a crucial role in the hydrogenation of FAL. In the hydrogenation of FAL, water acted as a co-catalyst and significantly influenced the selective transformation of FAL to FOL. Besides, water protonation could efficiently influence the FAL conversion over PtNi HNFs catalyst. This is due to the strong interaction between the water molecules and the surface of the PtNi HNFs catalyst, resulting in the dissociation of water molecules into H^+ and OH^- species. The produced H^+ is transferred from the catalyst surface onto a carbonyl group (-CHO), resulting in a H-assisted CO cleavage [39].

3.4. Effect of FAL concentration on hydrogenation of FAL

In the previous works, hydrogenation reactions were mainly performed at low FAL concentrations (less than 10 wt%). However, it is desirable to achieve better economics by using high FAL concentration in the industrial process. Considering this, hydrogenation reactions were performed with various FAL concentrations and the results were shown in Table 2. When the reaction was carried at 100 °C with 1 wt% FAL, 99% FAL conversion with 99% FOL yield was obtained (entry 1, Table 2). Later, with the increase of FAL concentration to 20 wt%, a decrease in FOL yield was observed (entry 2–4, Table 2). The hydrogenation reaction was with a good FOL selectivity but less FAL conversion at 20 wt% FAL concentration. Further hydrogenation reactions were carried with 40 wt% FAL concentration for 1 h, only 26% FAL conversion with 22% FOL yield was obtained (entry 5, Table 2). Increasing the reaction time to 2h, FAL conversion and

278 FOL yield increased to 42% and 32%, respectively (entry 6, Table 2). Further increasing
279 reaction time to 4 h, a small mount increases in FAL conversion and FOL yield was
280 observed (entry 7, Table 2). The low FAL conversion and FOL yield may due to the
281 competition adsorption of FAL and FOL on the catalyst surface, which hinder the
282 conversion of FAL. When the hydrogenation reaction was carried at 150 °C with 40 wt%
283 FAL, 75% FAL conversion with only 26% FOL yield was observed, indicating that side
284 reaction would be predominance at high temperature and high substrate concentration.
285 Polymerized mucky products were observed at high FAL concentration, suggesting the
286 main side reaction is the self-condensation of FAL at high temperature (150 °C). These
287 results suggested that it is better to perform hydrogenation reaction at low FAL
288 concentration and low temperature.

Table 2. The effect of FAL concentration on hydrogenation of FAL

Entry	FAL (wt%)	*T* (°C)	Time (h)	FAL Conv. (%)	FOL yield (%)
1	1	100	1	99	99
2	5	100	1	95	95
3	10	100	1	74	74
4	20	100	1	51	50
5	40	100	1	26	22
6	40	100	2	42	32
7	40	100	4	49	37
8	40	150	1	75	12

Reaction condition: Weight of catalyst, 0.1 g; IPA 20 mL; 1 MPa H_2 was charged at room temperature.

289 *3.5. Optimization of the reaction conditions and the reaction kinetic study*

290 To further understand the relationship between the active sites of PtNi HNFs catalyst
291 and their catalytic performance, contact time experiments were performed. To study the

intrinsic kinetic of the reaction, the hydrogenation reactions were conducted at a low reaction temperature (80 °C) and short reaction duration to avoid mass transfer limitations (Fig. 3A). It could be seen that the FOL yield increased significantly with an increase in the amount of catalyst from 40 mg to 100 mg. Further increasing the amount of catalysts to 130 mg led to a little decrease in FOL yield, which was attributed to the acetalization reaction of FAL with IPA. The effect of the number of active sites of catalysts on the FOL formation rate is described in Fig. 3(B). The reaction rate was measured by collecting FOL products at 10 min to avoid mass transfer limitations. A linear relationship between the reaction rate and the concentration of the active sites in PtNi HNFs catalyst was observed, suggesting the conversion of FAL is first order in respect to the concentration of the active sites, the adsorption and activation of the FAL molecule on the active sites is the rate-determining step. Various initial FAL concentrations were employed to study the effect of FAL concentration on their catalytic performance at 80 °C (Fig. 3C). The FAL conversion increased dramatically as the reaction time increased, and 99% FOL yield was obtained when the concentration of FAL was only 0.05 mol L^{-1}. Further increasing the concentration of FAL leads to a longer reaction time, which is attributed to the competitive adsorption of FAL and FOL.

The influence of the temperature on the hydrogenation of FAL to FOL over PtNi HNFs is also studied at various temperatures (60 °C to 120 °C). As shown in Fig. 3(D), the temperature showed a clear effect on the catalytic performance for the hydrogenation of FAL from 60 °C to 120 °C. When the reaction was carried at low temperature (60 °C) for 30 min, a low FOL yield (12.8%) was obtained. The FOL yield dramatically increased to 77.8% as the temperature increased to 100 °C. Furthermore, the FOL yield

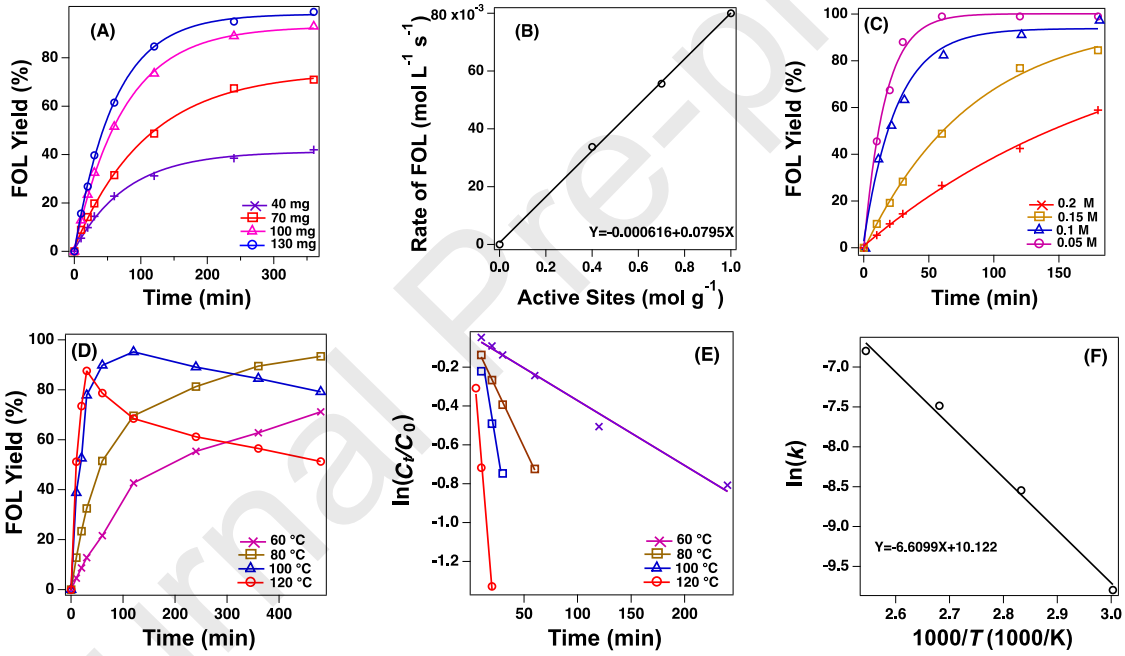

Fig. 3. (A) Effect of the amount of catalyst on the FOL yield. (B) Effect of the concentration of active site on the FOL formation rate of 10 min. (C) Effect of the concentration of FAL on the hydrogenation of FAL to FOL. (D) Effect of reaction temperature on the FOL yield. (E) Kinetic fit for the hydrogenation of FAL at different temperatures. (F) Corresponding Arrhenius plots for PtNi HNFs.

increased to 95.2% by increasing the reaction time to 120 min at 100 °C. However, the FOL yield gradually declined due to the acetalization of FAL with IPA with a further

increase temperature (120 °C) for 30 min. Therefore, 100 °C was selected for the hydrogenation of FAL in the following study. The rating formula of FAL conversion can be expressed by Eq. (1). We proposed that the hydrogenation of FAL is first order reaction (∂ =1) with respect to FAL concentration due to the fixed amount of catalyst and the excess of hydrogen donor. Therefore, Eq. (1) could be expressed as Eq. (2), where c_0 is the initial concentration of FAL and c_t is the concentration of FAL after a reaction time of t. At low FAL conversion (10 min), it is apparent to see that $\ln(C_0/C_t)$ follows a linear relationship with the reaction time (Fig. 3E). The reaction rate constants (k) were calculated by the corresponding slope of the plots, which are 5.56×10^{-5}, 1.94×10^{-4}, 5.61×10^{-4}, and 1.11×10^{-3} s^{-1} for temperature 60 °C, 80 °C, 100 °C, and 120 °C, respectively (Fig. 3F). Based on the Arrhenius plot (Eq. (3)), the apparent activation energy (E_a) was determined to be 54.95 kJ mol^{-1} over the PtNi HNFs for the hydrogenation of FAL into FOL.

$$-\frac{\mathrm{d}c(\mathrm{FAL})}{\mathrm{d}t} = kc(\mathrm{FAL})^{\partial} \quad (1)$$

$$\ln\frac{c_t}{c_0} = -kt \quad (2)$$

$$\ln k = \ln A - \frac{E_a}{RT} \quad (3)$$

3.6. Hydrogenation of other biomass-derived compounds

Besides the high activity of PtNi HNFs in the hydrogenation of FAL, the highly efficient hydrogenation of other biomass-derived platform compounds is also of excellent significance. As shown in Table 2, 5-hydroxymethylfurfural (5-HMF) and 5-methyl

Table 3. Results of PtNi HNFs hydrogenation of various carbonyl compounds to alcohols

Entry	Substrate	Product	Time (h)	*T* (°C)	Conv. (%)	Selec. (%)
1	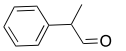	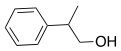	2	100	90	94
2	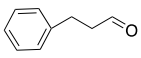	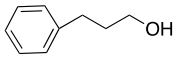	2	100	97	97
3	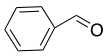	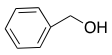	2	100	95	97
4		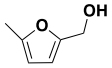	2	100	88	97
5		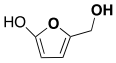	2	100	85	94
6		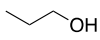	2	80	95	97
7	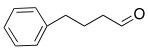	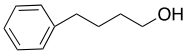	2	100	78	92
8	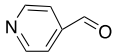	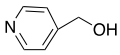	2	100	95	96
9	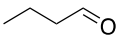	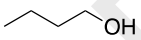	2	100	92	95
10	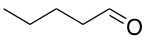	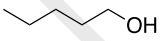	2	100	90	95

Reaction condition: 0.1 g substrates in 20 mL IPA, 0.1 g catalyst, 2 MPa H_2 at room temperature.

furfural are also important platform chemicals which are obtained from renewable biomass. PtNi HNFs also exhibited an excellent catalytic performance for the hydrogenation of 5-HMF and 5-methyl furfural. More than 90% reactant conversion was obtained with more than 95% product selectivity to the corresponding alcohol. The only by-product is the acetalization of reduced alcohol with IPA. The by-products could also be as a potential fuel additive due to their high energy density. Furthermore, the other substrates (Table 2) suggested that PtNi HNFs catalyst was a versatile catalyst for the

hydrogenation of commercial aldehydes to alcohols.

3.7. DFT calculation

To further understand the hydrogenation of FAL mechanism over PtNi HNFs, three different catalytic modes were investigated by density function theory (DFT), which includes pure Ni cluster, Pt cluster and PtNi (fcc) hollow nanoframes (Fig. 4). The detail DFT calculation is shown in Fig. S3. Initially, the adsorption step of FAL is spontaneous reaction on three models, especially the Ni catalyst releases the relatively biggest energy. This is because the empty *d* orbital of Ni atom is easily accepting the long pair electrons of carbon atoms. However, the catalytic surface will be poisoned by the intermediates if the activation energy is too strong from the Brønsted–Evans–Polanyi principle. Then, the last desorption step needs input massive energy (80.9 kJ/mol) on the Ni model. Compared to the two pure catalysts, the PtNi HNFs have compromised binding energy for FAL in the first step, owing to the Pt active site accepts extra electrons (0.18 eV) from Ni atom (Bader charge analysis). In the following step, the hydrogenation divides into two possible pathways: The Oxygen atom hydrogenated by a proton-coupled electron transfer (dash line), while the second is the first hydrogenation occurred on the carbon atom (solid line) [40,41]. Fig. 4 indicated that all dash lines are favor pathway in three catalytic models. Although the PtNi HNFs have bigger binding energy than the pristine Pt cluster, it holds the smallest FOL released energy in the last step. The main reason is that the Pt active locates the angle of PtNi HNFs, which separated by Ni atoms in the special

structure, while the FAL was adsorbed on the edge Pt atoms in the Pt catalyst. Therefore,

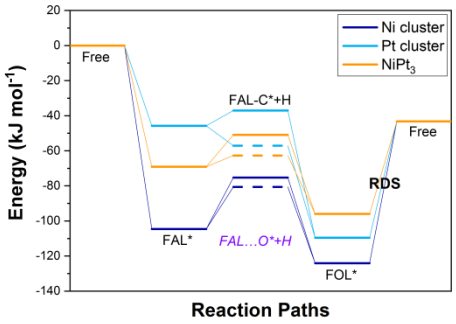

Fig. 4. Step-by-step hydrogenation mechanism of FAL to FOL on the Ni (111), Pt (111) and NiPt (fcc) hollow nanoframes surface. The dash line means the hydrogenation occur on the oxygen atom, and carbon atom reaction is solid line.

the last step is the rate-determining step (RDS) for three models and the PtNi HNFs have the best performance for FAL reduction reaction (49.93 kJ/mol).

3.8. Proposed mechanism

Both geometric and electronic structures determine the activity and selectivity of a bimetallic catalyst. In the hydrogenation of FAL, PtNi/C alloy catalyst showed high selectivity in total hydrogenation of FAL to THFA, while PtNi HNFs catalyst exhibited a high selectivity in FOL. This may due to the corresponding morphology of the solid polyhedral as revealed by TEM (Fig. 1). Ni exhibited a relatively homogenous distribution inside of the particles, whereas Pt was relatively concentrated at the edges [34]. The activity test suggested that Pt and Ni in a synergetic way facilitate promotion of the catalytic performance, which could be described by the adsorption mode of FAL and

the effect of electronic structure on the adsorption energy. There are two different adsorption patterns of FAL on metal catalysts, η_1 mode of FAL on Pt (Fig. S5A) and η_2 mode on Ni (Fig. S5B) [39]. A high FOL selectivity was obtained by Pt/C catalyst, which was attributed to the η_1 adsorption mode of FAL. However, only 34% FAL conversion was obtained, because Pt was predominantly present in the metallic state, the electron-rich Pt was difficult for the interaction between FAL and Pt, and thus restricted the adsorption of FAL on Pt surface. In our previous work, we proved that the adsorption of FAL was enhanced on PtNi alloy catalyst by in-situ FTIR [32]. Theoretical calculation suggested that alloying of Pt to Ni tuned the *d*-band structure of Ni and therefore changed the adsorption mode of FAL. The tilted orientation weakens the adsorption energy of furan ring on catalyst surface, which restricts the activation of furfuran ring and therefore enhances the selective to FOL. Among these adsorption patterns, the η_1 mode promoted the preferential reduction of the C=O bond and obtained the product FOL, while η_2 mode promote the total hydrogenation to THFA. Besides, the addition of Ni could enhance the adsorption of FAL. The XPS results indicated that some Ni atoms were present in Ni^{2+}, the electron-deficient Ni acted as Lewis acid site for the adsorption of the C=O bond through oxygen atoms, which essentially enhanced the adsorption of FAL (Fig. S5D) [40]. The morphology of PtNi HNFs catalyst may prevent the adsorption of FAL via η_2 mode on the surface of catalyst. The direct η_2 adsorption of FAL on inside Ni may be suppressed by edge Pt, which could promote the adsorption of FAL on edge Pt via η_1 adsorption mode, and therefore enhanced the FOL selectivity (Fig. S5D).

In Section 3, gas H_2 was demonstrated as a proton donor in the hydrogenation of FAL rather than solvent. Ni-base catalysts were excellent in the adsorption and activation of H_2, but the activated H* and intermediates were hard to desorb from the surface of Ni, which will slow the subsequent hydrogenation. The electronic structure of Ni (*d*-band) is the major factor in determining the desorption of H* and intermediates on Ni. Based on the DFT calculation, *d*-band center of Ni (−1.48 eV) downshifted to Pt-Ni-Pt (−2.74 eV), the addition of Pt to Ni decreased the desorption energy of FOL on Ni surface [26]. Besides, the heterolytic splitting of the gas hydrogen to H^+ and H^- could be enhanced by metallic Pt, which was concentrated at the edges of PtNi HNFs. The σ electrons of gas H_2 could be accepted by metal Pt occupied *d*-orbitals, which donated *d*-electrons to the σ^* antibonding orbital of gas hydrogen. Therefore, the H−H bond was weakened and easily to be cleaved, then H_2 was heterolytically dissociated to H^- and H^+. The high electron density of the Pt is beneficial for the hydrogenation of FAL due to the dissociation of H_2 which needs the donation of *d*-denotation of Pt to hydrogen.

3.9. Catalytic reusability

In order to demonstrate the catalyst is heterogeneous, the PtNi HNFs was filtered from the solution after 30 min at 100 °C. After that, the hydrogenation of FAL was allowed to react for another 3 h under identical conditions without PtNi HNFs catalyst (Fig. 5A). It can be seen that the FAL conversion is maintained. When the PtNi HNFs catalyst was reintroduced to the solution, a high FAL conversion (96.2%) was obtained

after 30 min. The extract Ni concentration in the mixture was detected to be 2.3 ppm while no Pt was observed via ICP, suggesting only small amount of Ni were leaching into the mixture. The results demonstrated that the heterogeneous character of PtNi HNFs and the hydrogenation of FAL could be effectively controlled by the remove or add of the PtNi HNFs catalyst.

The recycling experiments of PtNi HNFs for the hydrogenation of FAL were investigated by maintaining approximately 90% FAL conversion at 100 °C for 1 h. After the first experiment, the catalyst was separated by centrifugation and then washed with deionized water and dried at 60 °C overnight. Because of the loss of the catalyst, small scale experiments were investigated by keeping the same ratios of solvent, substrate and catalyst at every run. The results of recycling experiments are shown in Fig. 5(B). Only

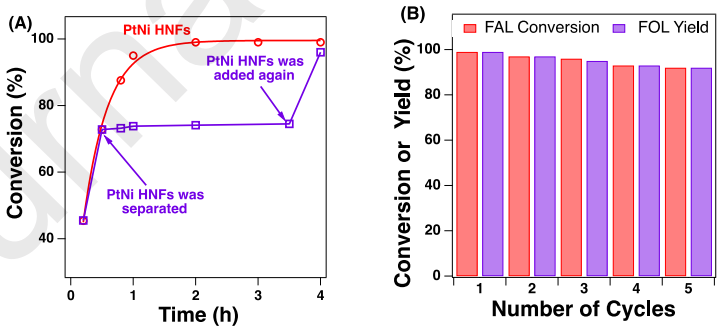

Fig. 5. (A) Heterogeneity and (B) reusability of PtNi HNFs catalyst. Reaction condition: weight of catalyst, 0.1 g; IPA 20 mL; 1 MPa H_2 was charged at room temperature.

slightly reduce of FOL yield after 5 cycles suggested that the catalyst had good stability. Furthermore, the used catalyst was characterized by ICP and XRD, no significantly metal leaching was observed (Fig. 2 and Table S1).

4. Conclusions

In summary, we have constructed a PtNi HNFs catalyst of which Ni was distributed inside of the particles, whereas Pt was concentrated at the edges. The resulting PtNi HNFs possessed a high activity in the hydrogenation of biomass-derived oxygenates and showed a higher TOF than Pt/C and Ni/C catalysts, especially for the selective hydrogenation of FAL to FOL. In this reaction, the hydrogen donor was gas hydrogen at low temperature while alcohols (IPA in this study) donated hydrogen at high temperature. The kinetic study suggested the activation energy was as low as 54.95 kJ mol^{-1}. DFT calculation suggested the desorption of FOL is the rate-determining step and PtNi HNFs have compromised binding energy for FAL compared with Ni cluster and Pt cluster, which will promote the desorption of FOL and thus enhanced the catalytic performance. Mechanism study indicated that the Ni was distributed inside of the catalyst, which worked as Lewis acid to enhance the adsorption of the C=O bond and the heterolytic dissociation of hydrogen was facilitated by the edge Pt. Understanding the effect of geometric and electronic structure of PtNi catalysts on the selectivity of FAL hydrogenation could guide for future hydrogenation catalyst design.

Acknowledgments

This work is financially supported by the National Key R&D Program of China (No. 2019YFD1100601), the National Key R & D Program of China (2018YFB1501500), the National Natural Science Foundation of China (Nos. 51776206 and 51536009), the Local Innovative and Research Teams Project of Guangdong Pearl River Talents Program (2017BT01N092) and the "Transformational Technologies for Clean Energy and Demonstration", the Strategic Priority Research Program of the Chinese Academy of Sciences (No. XDA21060102).

References

[1] E.L. Kunkes, R.M. West, J.C. Serrano-Ruiz, C.A. Gärtner, J.A. Dumesic, Science 322 (2008) 417-421.

[2] D.M. Alonso, M.A. Mellmer, E.I. Gurbuz, J.A. Dumesic, Energy Environ. Sci. 6 (2012) 76-80.

[3] Y.D. Wang, N. Yan, Chem. Commun. 52 (2016) 6210−6224.

[4] N. Shi, Q. Liu, Q. Zhang, T. Wang, L. Ma, Green Chem. 15 (2013) 1967-1974.

[5] R.V. Karinen, K. Niemela, ChemSusChem 4 (2011) 1002-1016.

[6] S. Liu, J. Fu, K. Alexopoulos, B. Saha, D.G. Vlachos, ACS Catal. 9 (2019) 7679-7689.

[7] H.J. Cho, B. Xu, ACS Catal. 10 (2020) 4770-4779.

[8] S. Fang, Z. Cui, Y. Zhu, C. Wang, J. Bai, X. Zhang, Y. Xu, Q. Liu, L. Chen, Q. Zhang, L. Ma, J. Energy Chem. 37 (2019) 204-214.

[9] S. Climent, M. Iborra, Green Chem. 13 (2011) 520-540.

[10] S. Climent, M. Iborra, Green Chem. 16 (2014) 516-547.

[11] C. Ji, G. Yang, Z. Pang, ACS Sustain. Chem. Eng. 11 (2018) 15306-15315.

[12] W. Gong, R. Fan, H. Zhang, G. Wang, H. Zhao, Fuel 231 (2018) 165-171.

[13] B. Chen, Z. Huang, G. Yuan, J. Energy Chem. 25 (2016) 888-894.

[14] M.J. Gilkey, B. Xu, ACS Catal. 6 (2016) 1420-1436.

[15] F. Toledo, C. Sepúlveda, R. García, J.L.G. Fierro, A.Videla, R. Serpell, N. Escalona, Fuel 242 (2019) 532-544.

[16] K. Yan, Fuel 115 (2014) 101-108.

[17] Z. Huang, B. Kevin, J. Dumesic, J. Huber, ACS Sustain. Chem. Eng. 6 (2017) 4699-4706.

[18] L. Zhang, A. Wang, T. Zhang, Chem. Rev. 120 (2019) 683-733.

[19] K. Yan, T. Lafleur, C. Jarvis, Renew. Sustain. Energ. Rev. 38 (2014) 663-676.

[20] S. Nandi, P. Patel, N.H. Khan, R.I. Kureshy, A.B. Panda, ACS Appl. Mater. Inter. 10 (2018) 24480–24490.

[21] F. Tang, M.D. Walle, A. Mustapha, Y.N. Liu, J. Catal. 383 (2020) 172-180.

[22] Z. Jiang, Z. Lin, J. Xie, J.Chen, ACS Catal. 7 (2017) 5758–5765.

[23] K. Yan, A. Khorshidi, V.A. Sethuraman, A.A. Peterson, P.R. Guduru, Angew. Chem. Int. Ed. 55 (2016) 6175–6181.

[24] L. Zhang, G. Gao, X. Yan, N. Chen, J. Chen, M. Soo, B. Wood, D. Yang, A. Du, X. Yao, Chem 4 (2018) 285–297.

[25] D. Voiry, K.P. Loh, M. Chhowalla, Nat. Rev. Chem. 2 (2018) 01-05.

[26] M. Humbert, J. Catal. 297-306 (2008).

[27] X. Zhao, Z. Fang, J. Ding, W. Sang, Y. Wang, J. Zhao, Z. Peng, J. Zeng, J. Am. Chem. Soc. 137 (2015) 2804–2807.

[28] Z. Li, Y. Wen, Y. Gao, X. Xing, Z. Wei, H. Sun, Y.W. Zhang, W. Song, ACS Catal. 9 (2019) 5084–5095.

[29] Y. Yang, Y. Chen, W. Liu, H. Feng, B. Wang, X. Zhang, M. Wei, Green Chem. 21 (2019) 5352–5362.

[30] F. Tang, G. Zhang, M. Zhang, Y.N. Liu, Ind. Eng. Chem. Res. 58 (2019) 5543–5551.

[31] J. Wu, J. Li, P. Sun, X. Long, F. Li, Appl. Catal. B Environ. 203 (2017) 227-236.

[32] J.C. Wu, Q. Chen, L. Chen, Q. Liu, C.G. Wang, L.L. Ma, Energy Fuel 34 (2020) 2178–2184.

[33] Y. Yang, Q.Y. Liu, D. Li, J. Tan, Q. Zhang, C.G. Wang, L.L. Ma, RSC Adv. 7 (2017) 16311–16318.

[34] C. Chen, Z. Huo,Z. Zhu,W. Huang, H.L. Xin, J.D. Snyder, D. Li, J.A. Herron, M. Mavrikakis, M. Chi, K.L. More, Y. Li, N.M. Markovic, G.A. Somorjai, P. Yang, V.R. Stamenkovic, Science 343 (2014) 1339-1343.

[35] J. Zeng, J. Power Sources 140 (2005) 268-273.

[36] B.S. Stamenkovic, K. Mayrhofer, P.N. Ross, N.M. Markovic, J. Rossmeisl, J. Greeley, J.K. Norskov, Angew. Chem. Int. Ed. 45 (2006) 2897-2901.

513 [37] S. Kulkarni, A. Patel, J.K. Norskov, Chem. Rev. 118 (2018) 2302−2312.

514 [38] S. Zhou, Z. Xiang, T. Song, D. Liu, F. Lu, H. Qi, Appl. Catal. B Environ. 248 (2019)

515 31-43.

516 [39] M. Dohade, P. Doepe, Green Chem. 19 (2017) 1144.

517 [40] H. German, M. Sheintuch, J. Phys. Chem. C 117 (2013) 7475−7486.

518 [41] S. Sitthisa, T. Ma, Y. Balbuena, D. Resasco, J. Catal. 277 (2011) 1-13.

519

520 Graphical abstract

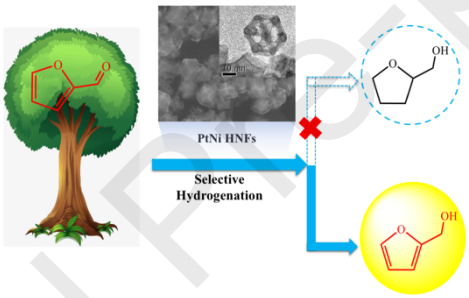

521

522 Selective and efficient upgrading of furfural over controllable PtNi bimetallic catalyst
523 under mild conditions